DOI 10.4467/21995923GP.22.010.17088 GEOINFORMATICA POLONICA
21: 2022

Rafał Gawałkiewicz[1]
ORCID: 0000-0003-4261-1697

IT AND SURVEYING TECHNOLOGIES IN GEO-HAZARDS MODELING OF HISTORIC ANTHROPOGENIC OBJECTS ON THE EXAMPLE OF THE WANDA MOUND IN KRAKOW

[1] AGH University of Science and Technology, Faculty of Mining Surveying and Environmental Engineering Kraków, Poland
gawalkie@agh.edu.pl

Abstract

Over the recent ten years the development of geodesic and informatic tools contributed to enrichment of measurement and interpretation methods as well as visualization of various anthropogenic and natural objects subdued to deformations over the time. The availability of photogrammetric methods (terrestrial and airborne measurements) caused that they are widely applied in monitoring of various objects subdued to the external (i.e., atmospheric) factors (rain, wind, temperature), mining (influence of underground mining). This also refers to natural terrain surface affected by mass movements and artificial earth constructions (mounds, spoil tips, dikes, road and rail embankments), the changes of which can threaten stability and pose threat to objects situated in these areas/objects and their users. There are many methods of getting spatial data and their processing, allowing the interpretation of geological threats. The article presents the measurement and interpretation model of the changes of artificially formed area with the historic Wanda Mound in Krakow with the use of robotic station SPS 930 Trimble and active signal MT 1000 and program AutoCAD v. 2021 (splines Coons patches). In the article it was shown that applying a limited number of the data set elements in a definite geometric system and the same measurement technology in the studied period of the analysis (2013–2022), it is possible to record and graphically interpretate changes on the surface of an earth mound, manifested in the phenomenon of ground creep, even in case of small values.

Key words: geological threat to historic objects, the Wanda Mound, 3D modelling of geological threat

INFORMATYCZNE I GEODEZYJNE TECHNOLOGIE W MODELOWANIU GEOZAGROŻEŃ ZABYTKOWYCH OBIEKTÓW ANTROPOGENICZNYCH NA PRZYKŁADZIE KOPCA WANDY W KRAKOWIE

Abstrakt

Rozwój narzędzi geodezyjnych i informatycznych przyczynił się w ostatnim dziesięcioleciu do wzbogacenia metod pomiarowych i interpretacyjnych oraz wizualizacji różnego rodzaju obiektów pochodzenia antropogenicznego oraz naturalnego, które podlegają deformacjom w czasie. Dostępność metod fotogrametrycznych (pomiary naziemne i lotnicze) sprawiła, że wykorzystywane są one powszechnie do monitoringu różnego rodzaju obiektów poddanych oddziaływaniu czynników zewnętrznych, tj. atmosferycznych (deszcz, wiatr, temperatura), górniczych (wpływ podziemnej eksploatacji górniczej). Dotyczy to także naturalnych powierzchni terenu objętych ruchami masowymi oraz sztucznych budowli ziemnych (kopce, hałdy, groble, nasypy drogowe i kolejowe), których zmiany mogą zagrażać stateczności i stwarzać zagrożenie dla obiektów towarzyszących, usytuowanych na tych obszarach/obiektach oraz ich użytkowników. Istnieje szereg metod pozyskiwania danych przestrzennych oraz ich opracowania, pozwalających na interpretację geozagrożeń. W artykule przedstawiono model pomiarowy oraz interpretacyjny zmian sztucznie ukształtowanej powierzchni zabytkowego Kopca Wandy w Krakowie, przy wykorzystaniu stacji robotycznej SPS 930 Trimble i sygnału aktywnego MT 1000 oraz programu AutoCAD v. 2021 (funkcje sklejane oraz płaty Coons'a). W artykule dowiedziono, że stosując ograniczoną liczebność zbioru danych w określonym układzie geometrycznym oraz tę samą technologię pomiarową w rozpatrywanym okresie analizy 2013–2022, możliwa jest rejestracja oraz graficzna interpretacja zmian powierzchni ziemnego kopca podlegającej zjawisku spełzywania gruntu, nawet w przypadku niewielkich wartości.

Słowa kluczowe: geozagrożenia obiektów zabytkowych, Kopiec Wandy, modelowanie przestrzenne geozagrożeń

1. INTRODUCTION

Deformations of the surface in the area of Poland are monitored in the framework of the task of the State Geological Service (Polish: Państwowa Służba Geologiczna) using satellite radar interferometry InSAR [1]. These studies mainly refer to large area unites [2], i.e., areas of mining hard coal, lignite, ores of copper, zinc and lead, exploitation of gas, as well as post-mining areas (mainly salt deposits). Due to high resolution of SAR (Synthetic Aperture Radar), guaranteed by satellite TerraSAR-X, it is possible to cover the area in SpotLight mode with resolution 1.3 m [2].

Basic accuracy criterion of the Numeric Terrain Model, which is base material for the analyses of the surface morphology and its change in time is vertical component H, the accuracy of which is determined by the designation of final product. According to American accuracy standards [3] „basic" accuracy of Numeric Terrain Models (NMT – defined for open flat areas), described with contour interval 0.5 m, oscillated on the level of RMSE error ±46.0 mm (checked on the confidence level 95%). And the accuracy of positioning a horizontal point for the most accurate scale 1:1200 is defined on the level of RMSE error = ±67.0 cm.

In case of the observations of geological threat to historic monumental mounds in Krakow in the option of registering structural deformations with the use of terrestrial laser scanning and electronic total stations, the works were carried out on the Piłsudski Mound and Krakus Mound [4, 5, 6].

Morphometric analyses of natural areas, but especially anthropogenic objects of small area (considered in microscale), as well as historic monumental mounds in Krakow, documenting geometric changes in the framework of the observations of mass movements, due to their characteristics (mainly creep) and magnitude, it is required to apply precise measurement methods. Thus, the monitoring is conducted based on the network of control points (deformation determined based on discrete points) permanently stabilized in ground, when the values of their horizontal dislocations are obtained with the polygonization method and vertical dislocations – by precise levelling method, referring to the points of the retailing network. Such a way of analysis based on a limited number of points does not guarantee full characteristics of a phenomenon connected with the dislocation of earth masses in time. Thus, an alternative for geometric observations of the changes in natural and artificial surfaces can be structural monitoring carried out with the application of robotic stations with the preservation of a defined measurement scheme (profile) and information-mathematic tools, allowing the construction of 3D models in a uniform system of spatial coordinates. This gives the possibility of easy comparison between the state of the object over in various time intervals. It is important to choose proper methodology of the measurement and interpretation model for the predicted values of geometric changes of the object in time.

The historic Wanda Mound in Krakow has been showing slow mass movements such as downhill creep and slide, although up till now its landslide card in the framework of SOPO PIG has not been made.

The article presents the results of the modelling of the earth top of the Wanda Mound, based on total station measurements with the application of vertical profiles (safe and direct access to the surface) and information tools (splines and Coons patches), which allow visualisation of the construction, preserving high accuracy of the 3D model.

2. METHODS OF FIELDWORK AND DATA ACCURACY ANALYSIS

Nowadays, one of leading measurement methods that made revolution in the methodology of obtaining data on physical surface of the Earth in the framework of GIS have become LiDAR (Light Detection and Ranging) technology recording topographic data in terrestrial, airborne and mobile version [7, 8].

Smaller areas are usually observed and recorded with the use of LiDAR (Light Detection and Ranging) technology, which guarantees high resolution and relatively high accuracy of the positioning of the points on the surface. In the carried out in Poland large projects, among others ISOK, the final product is the cloud of points ALS of density 6 points/m^2 (for priority areas) and 12 points/m^2 for cities above 50 000 residents, with the accuracy of horizontal positioning (mean error of ALS point cloud after equalization) on level $m_P \leq \pm 0.10$ m and height positioning $m_H \leq \pm 0.40$ m [9]. Research studies with the use of LiDAR technology conducted in the city of Krakow within the area of the University of Agriculture and the Wawel Hill by Borowiecki and Ślusarski [10], allowed us to estimate the error of $RMSE_{(H)}$ in the vertical plane on the level $RMSE_{(H)}$ = ±17–19 cm, and in the level $RMSE_{(XY)}$ = ±33–37 cm.

LIDAR technology is applied in the recording of artificially made and natural surfaces of the relief forms, both those accessible for direct measurements (electronic total stations), as well as difficult to access (high spoil tips and dikes, mounds, landslides, cavities). However, this requires the application specialist programs for quantitative, qualitative, and visual analysis of the point cloud. The analysis of measurement noise being the effect of signals disturbance (multiple reflections), makes an important stage of the preparation of data to a proper process of the modelling of the object. According to Borkowski I. [11] 95% of noise is automatically removed, but 5% must be removed in manual edition, which significantly increases the costs of airborne technologies. Natural surfaces, covered by vegetation, especially of variable density and height can affect the quality of the obtained point cloud. The qualitative analysis of this type of data requires their specialist processing in analytic and graphical programs.

The alternative to airborne technologies on accessible objects is electronic surveying with the application of total stations with an active prism, which minimises the impact of measurement errors (aiming, change in the inclination of the pole during the measurement lasting several seconds) influencing spatial positioning of the prism – and consequently – deformations of the generated 3D model. Actually, the connection of spatial data obtained in strictly defined measurement scheme (profile) and mathematical and information tools available in popular programs of CAD environment, can make an alternative for airborne technologies, especially repetitive measurements, carried out in the framework of geodesic monitoring.

The measurements of the mound geometry were made with the set consisting of the robotic precise total station SPS 930 Trimble (basic parameters of the instrument were put in table 1) and active signal MultiTrack 1000 (MT 1000).

In the framework of the optimization of measurement processes, Trimble developed a system of tracking reflectors, so-called **MultiTrack**. This system facilitates selection of a definite type of the goal, i.e., active or passive. Set MT 1000 is dedicated to total stations equipped in system Autolock. The original author's solution by Trimble in set MT 1000 is double belt of diodes (iden-

Table 1. Basic technical parameters of total station SPS930 Trimble applied in the measurements of control lines and observation networks in the area of the studied mounds

Tabela 1. Zestawienie podstawowych parametrów technicznych tachimetru SPS930 Trimble wykorzystanego do pomiarów osnów i sieci obserwacyjnych w rejonie badanych kopców

Parameter / Parametr		Value / Wielkość
The range of the distance measurement		2500 m
Maximal range of the distance measurement in the reflectionless mode		>600 m
Accuracy of the distance measurement in the mode of the prism measurement		±2 mm +2 ppm
Accuracy of the distance measurement in the mode of reflectionless measurement		±2 mm +2 ppm
The time of the measurement		3.2 sec.
Measurement accuracy of angles	horizontal	1” (0.3 mgon)
	vertical	1” (0.3 mgon)
Controller		TSC3
Magnification of telescope		30x

tifiers of the reflector). Localized in rings over and under the set of mirrors, diodes, sending signals of eight different frequencies in the direction of the instrument, allow precise positioning of the cross of the telescope towards the „centre" of geometric set both in horizontal and vertical planes. The user can at the same time control this process, as well as view the whole situation from the position of the instrument or navigate. The application of the active signal allows the automation of the measurement process. For the given integrated frequencies of the active prism and robotic total station, the instrument spontaneously „seeks" the centre of geometric active signal MT10000 Trimble'a, which eliminates the aiming error (human factor).

Thus, the user, by observing through the telescope the image of the cross and the outline of the signal, can observe the phenomenon of moving both elements towards each other by the value of vector *e* (figure 2). This translocation is especially visible in a vertical plane, while the value of vector e depends on the angle of the inclination of the line. According to the specifications by Trimble, the maximal linear error of automatic aiming of the cross does not exceed ±2 mm for the distance of 200 m, that – by the calculation into the values of an-

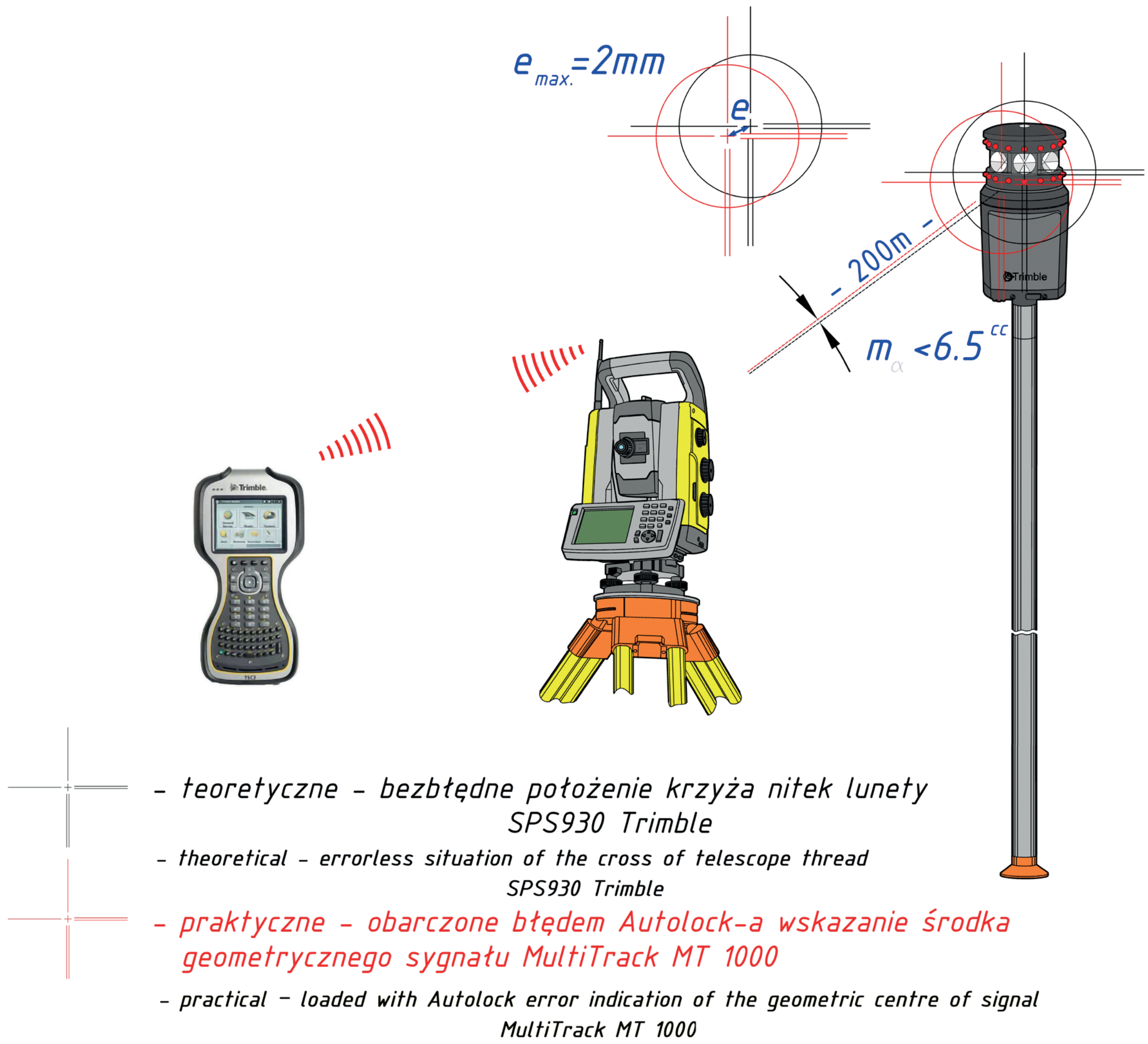

Fig. 1. Scheme of the work of the measurement set: total station SPS930 Trimble (fixed on the robotic pole – Trimble I.S. Rover) and the principle of functioning Autolock in the working mode with active signal MultiTrack MT1000

Ryc. 1. Schemat pracy zestawu pomiarowego: tachimetr SPS930 Trimble (zamocowany na robotycznej tyczce – Trimble I.S. Rover) and zasada działania funkcji Autolock w trybie roboczym z sygnałem aktywnym MultiTrack MT1000 gular translocation – angular error m_α does not exceed $\pm 6.5^{cc}$. The scheme of the work of the measurement set: total station SPS930 Trimble steered from the level of the controller TSC3 (fixed on the robotic pole – Trimble I.S. Rover) and the principle of function Autolock in the working mode with the active signal MultiTrack MT1000 is illustrated in figure 1.

To increase the accuracy during the picket measurement, the user can limit the impact of the fluctuations of signal during several seconds' angular and linear measurement, establishing the parameters of measurement protocol given by standard deviation for the value of the horizontal angle and length. This means that, if during the multiple recording and counting the values of the angle and length a slight increase of standard deviation σ occurs, above the user-accepted values, the prolongation of time measurement to obtain the established accuracy parameters or breaking the measurements without recording the data. During the inventory and control measurements, the standard deviation for angles was $\sigma_\alpha = \pm 3^{cc}$, while for distance $\sigma_d = \pm 2$ mm.

Since the total station measurements are carried out in one telescope situation, the possible impact of the instrument errors (inclination and collimation and linear error of the recognition of the geometric signal MT 1000 given by vector *e*) will have decisive influence on the accuracy of point positioning in profiles, thus test measurements were made. To make full accuracy characteristics of the robotic measurement set for determining the height of the point (or height difference), regarding the components of error $m_{\Delta H}$ (errors: instrumental, measurement of the height of the instrument and signal and height of the control line point), the measurement base on the slopes of the Krakus Mound was used. The base consisted of 44 stabilized points making 2 profiles, the height was defined with the use of precise levelling (DiNi12 + invar lath LD23). Defining the accuracy characteristics, in high range of the zenith angle of the measurement set (robotic station and MT1000 signal) was based on the theory of the true error. The carried-out test allowed defining error $RMSE_{(H)}$ in the level of ±2.6 mm.

The accuracy of the positioning the point on the topographic surface is also affected by the deviation of the signal fixed on the pole during the angular-linear measurement (figure 3). If assumed that angle a, the value of the advantage level (α =10') generates linear value higher than the value of the distance measurement error, then angle a is accepted as the parameter of the analysis of the topographic point coordinates. Thus, if 3α = 30' was accepted for the analysis, the value of height deformation (according to figure 2) is defined from the formula:

$$a = h_r \cdot (1 - \cos\alpha)$$

where:

h_r – the height of the active signal MT1000 Trimble (h_r = 2.0 m);

3α – triple value of the advantage of bull's eye level, is a = 0.1 mm, which is a negligible (non-significant) value.

In case of horizontal areas, inclination of the return signal does not impact on the vertical component in the assumed range. The deviation of the signal increases the linear value of the horizontal positioning. Only in case of horizontal positioning of points in relatively horizontal zones the influence of signal deviation has no major significance.

The influence of the inclination of the pole with the return signal on marking the vertical component grows with the increase of the inclination angle of the measured area, according to the formula:

$$b = \pm h_r \cdot \sin\alpha \cdot tg\,\beta$$

where:

β – inclination angle of the terrain surface in the measurement point.

This means that in case of the Wanda Mound, where mean slope inclination is 22.4° (in November 2022), the value of linear deformation of the vertical component H is b = ±7.2 mm, and of the horizontal component c (downhill/uphill, as in fig. 2) 17.5 mm.

The accuracy vertical coordinate H of any point of the topographic surface is formed independently from the mentioned components *a* and *b,* also measurement errors:

- height of the stand of the total station m_{st} (control line point), which does not exceed values m_{st} = ±0.3 mm (precise levelling);
- height of the instrument (on the stand) m_{hi} (in case of precise measurements the assumed value is m_{hi} = ±1 mm);
- height of signal m_{hr} (in case measurements of precise measurements the assumed value is m_{hr} = ±1 mm),

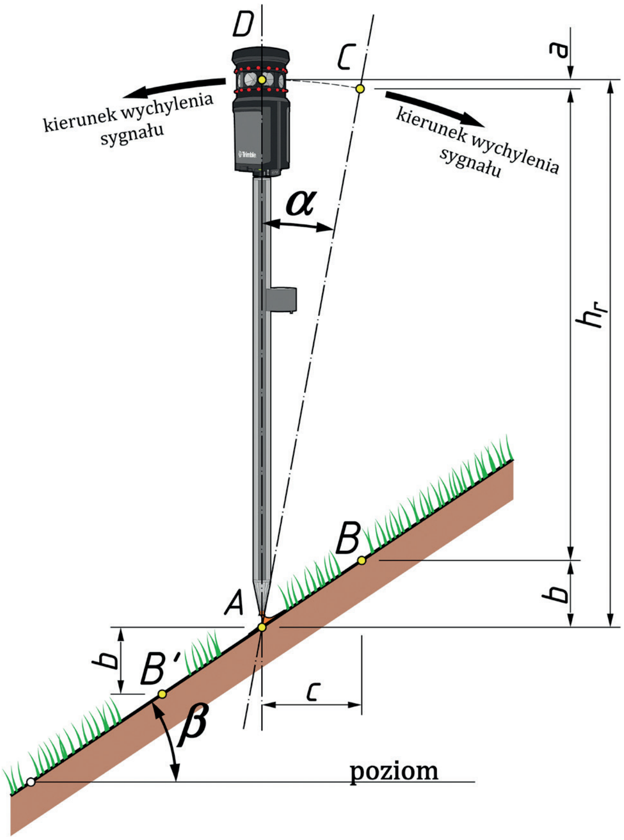

Fig. 2. The influence of signal inclination on the positioning of the topographic point

Ryc. 2. Wpływ wychylenia sygnału na pozycjonowanie punktu topograficznego

which for the accepted measurement scheme (measurement without changing the height signal) take the character of systematic errors.

3. METHODS OF CARTOGRAPHIC WORKS AND ACCURACY ANALYSIS OF THE 3D MODEL

For many years, in constructing models of objects and surface of irregular geometry or networks TIN are used [4, 12], direct measurements on points of variable density (terrestrial measurement) or relatively uniform (airborne measurement) or regular networks GRID generated indirectly in interpolation programs based on the sets of the measurement data.

More and more often applied procedure of constructing models of 3D objects of high morphological variability is the application of advanced mathematical procedures based on approximation spline function [13, 14, 15, 16] and surfaces of second degree, the task of which is change of the point model into the area model. Thus, a common way of the projection of complicated geometry of point-measured coating structures is a form of connecting splines making a skeleton and interpolation grids, which made its „stuffing". The modelling of this type is often used in case of refrigerators, chimneys, bowls of radio-telescopes and amphitheatres, gas and liquid tanks, shaft furnaces, etc. Such models serve not only clear visualization of the object, but in practice, first of all to the assessment of the degree of deformation compared to the project data or previous measurement series (repetitiveness of measurements).

Constructing of the skeleton of the measured area with the help of splines gives the possibility of:

- description of local deformations;
- quick construction of the grid (network) model;
- obtaining a smooth model, complied with real form of the object or the construction of discontinuity edges, where required;
- in case of control measurements, comparison of strains, also beyond the marked points of point model;
- easy modification of the model in selected zones (based on updating a selected fragment of the area) without the need to reconstruct the whole skeleton;
- geometric description of the inventoried complicated spatial forms with only one model of spline;
- obtaining high accuracy of the full skeleton – grid model on the condition of relative regularity of the distribution of points on the surface (proper selection of the measurement model for the characteristics of the object based on the profile or regular grids of points).

Filling the skeleton with interpolation grids projecting actual area of the object allows:

- in case control measurements, determining the values of strains in any point of the construction, not necessarily the measured one;
- rendering facilitating a 3 form of the object presentation.

The advantage of using the robotic total station and active signal in the inventory of earth-made objects ac-

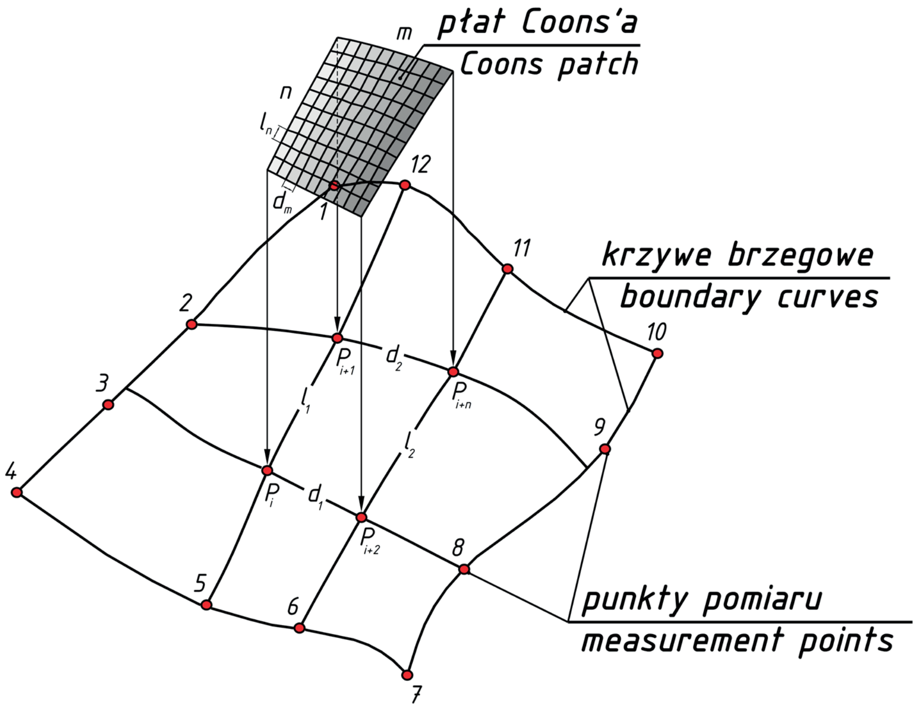

Fig. 3. Assumed structure of the shell model based on splines and Coons patches
Ryc. 3. Przyjęta zasada budowy modelu powłokowego w oparciu o krzywe sklejane oraz płaty Coons'a

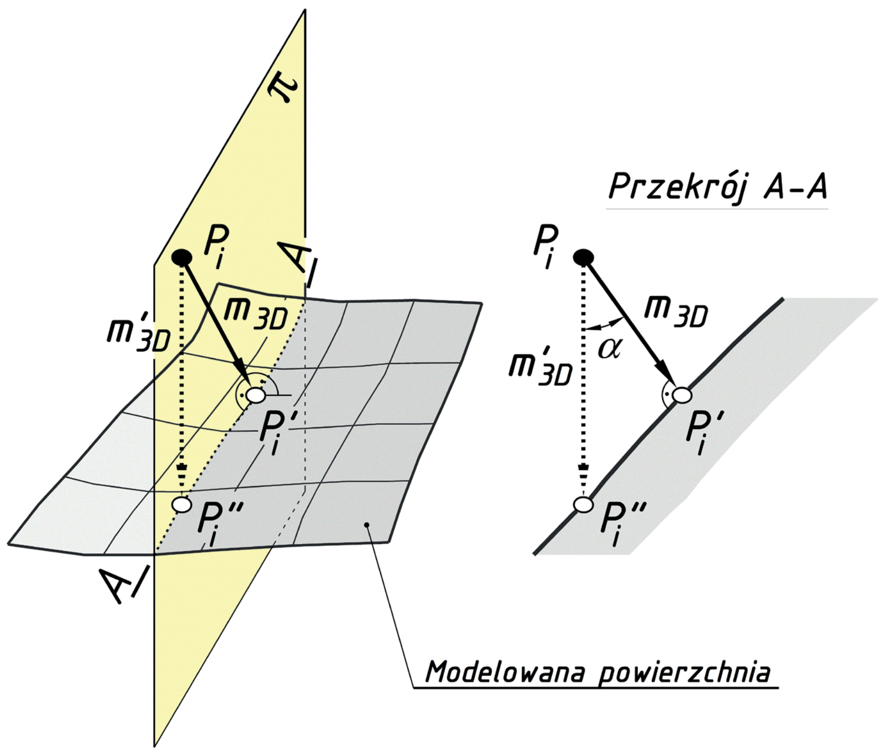

Fig. 4. Accepted principle of determining the modelling error m_{3D} based on the control point
Ryc. 4. Przyjęta zasada wyznaczania błędu modelowania m_{3D} na podstawie punktu kontrolnego

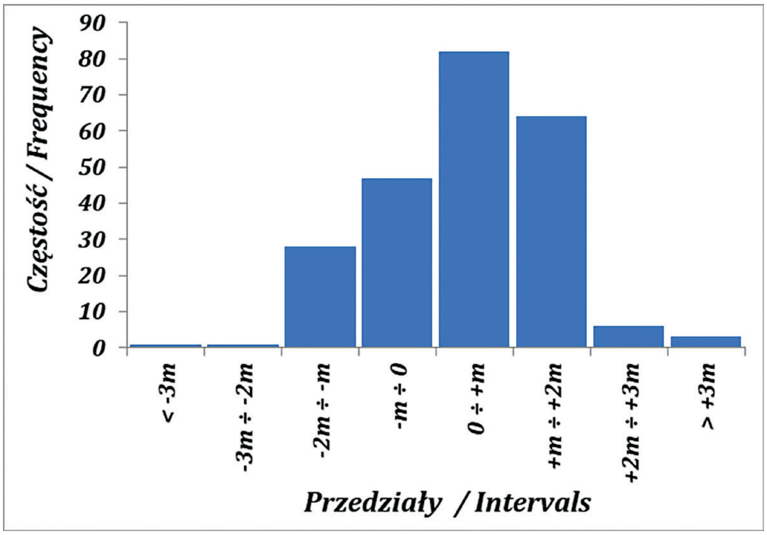

Error interval	Percentage [%]
< –3m	0.4
–3m ÷ –2m	0.4
–2m ÷ –m	12.1
–m ÷ 0	20.3
0 ÷ +m	35.3
+m ÷ +2m	27.6
+2m ÷ +3m	2.6
> +3m	1.3

Fig 5. Histogram (negative asymmetry) of the distribution of errors in the modelling of the topographic surface of the Wand Mound (where: $m = RMSE = \pm 39.4$ mm)

Ryc. 5. Histogram (asymetria ujemna) rozkładu błędów modelowania powierzchni topograficznej Kopca Wandy (gdzie: $m = RMSE = \pm 39.4$ mm)

cessible to direct measurement (possibility for the surveyor to walk on the object) is precise defining of the topographic area in a point, without the need of data filtration (removal of noise resulting from the influence of low vegetation on the accuracy of the measurement distance), accepting a definite scheme if generalization and smoothing the model. The geometry of the object was decisive in accepting the measurement model based on the radiant layout of the vertical profiles distribution – figure 6).

The development of splines based on the measured points in profiles made the main skeleton of the object in a vertical plane. Additionally splines of the contour character connected with previously drawn splines of vertical profiles or points of direct measurement (profiles) situated on established heights, were introduced. On the contacting edges of generated quadrangles bicubic surfaces, i.e., Coons patches were situated [16], as illustrated in figure 3.

For qualitative parameterization of the model, i.e., defining the accuracy of the topographic sufrace, RMSE value (square root of mean square error) was applied according to the formula:

$$RMSE = \sqrt{\frac{\sum_{i=1}^{n}\left(P_i - P_i'\right)^2}{n}} = \pm 39.4 \text{ mm}$$

where:

P_i – situation of the control point;

P_i' – projection of the control point on the surface of the model of the value m_{3D};

n – number of points control points n = 232.

The basis for the analysis was spatial data of 232 control points of the dispersed points characteristics. The distribution of control points was illustrated in figure 6. Based on the analysis of the distance of the control point to the generated surface (scheme presented in figure 6) with the use of the skeleton curves (splines) and Coons patches in AutoCAD, a hypsometric map of topographic deviations was made, which was visualized in figure 7. The histogram presenting the distribution of errors, accepted error intervals and percentage participation of errors in the sample were presented in figure 5.

4. ANALYSIS OF GEOMETRIC CHANGES IN THE MODEL

The point data XYH obtained with an electronic total station in the system of vertical profiles radiantly distributed in two measurement series (November 2013 and November 2022 – figure 7), gave bases for the con-

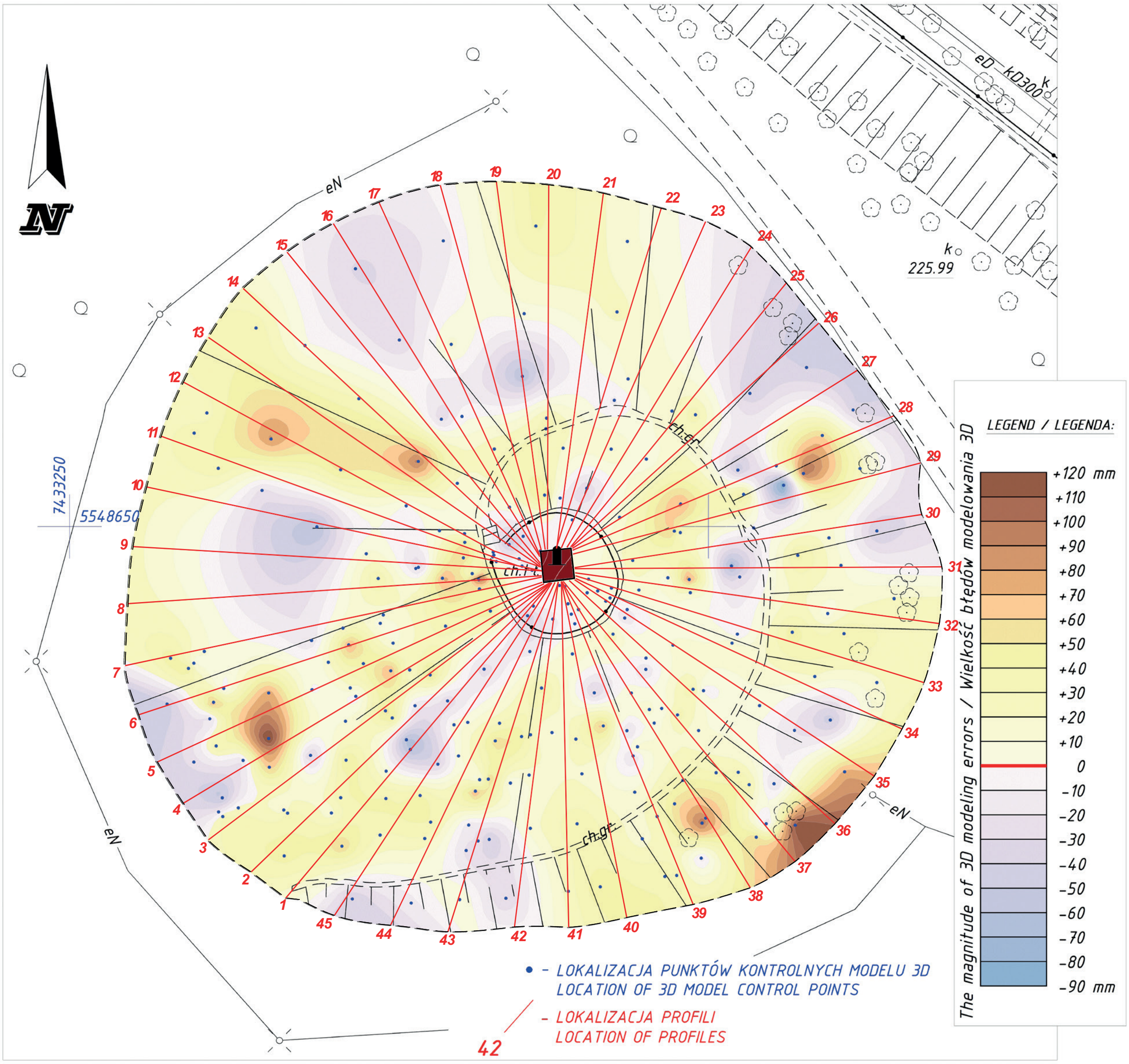

Fig. 6. Hypsometric map of the modelling of the error on the surface of the Wanda Mound – state of November 2022
Ryc. 6. Mapa hipsometryczna błędów modelowania powierzchni Kopca Wandy – stan na XI.2022 r.

clusion on the magnitude and directions of the changes in the earth coating of the Wanda Mound.

The purpose of the inventory was proving the usefulness of the construction of the 3D model of the historic Wanda Mound based on the vertical profiles (distribution of profiles was illustrated in figure 8). The profiles were supplemented by the points defining discontinuity of the surface, characteristic for the geometry of the object, such as verges: scarps, spiral path leading to the summit and the viewing gallery.

The mapping of the content of situation maps (figure 8) based on the codes of points or field sketches, allows the definition of horizontal translocations of characteristic elements of the mound. Overlapping of two images in a uniform system of spatial coordinates illustrate the values of vectors and directions of main dislocations of characteristic elements. The highest values of dislocations (the effect of the landslide and downhill creep of the earth mass) recorded in the direction ENE, where dislocation vectors achieved the values:

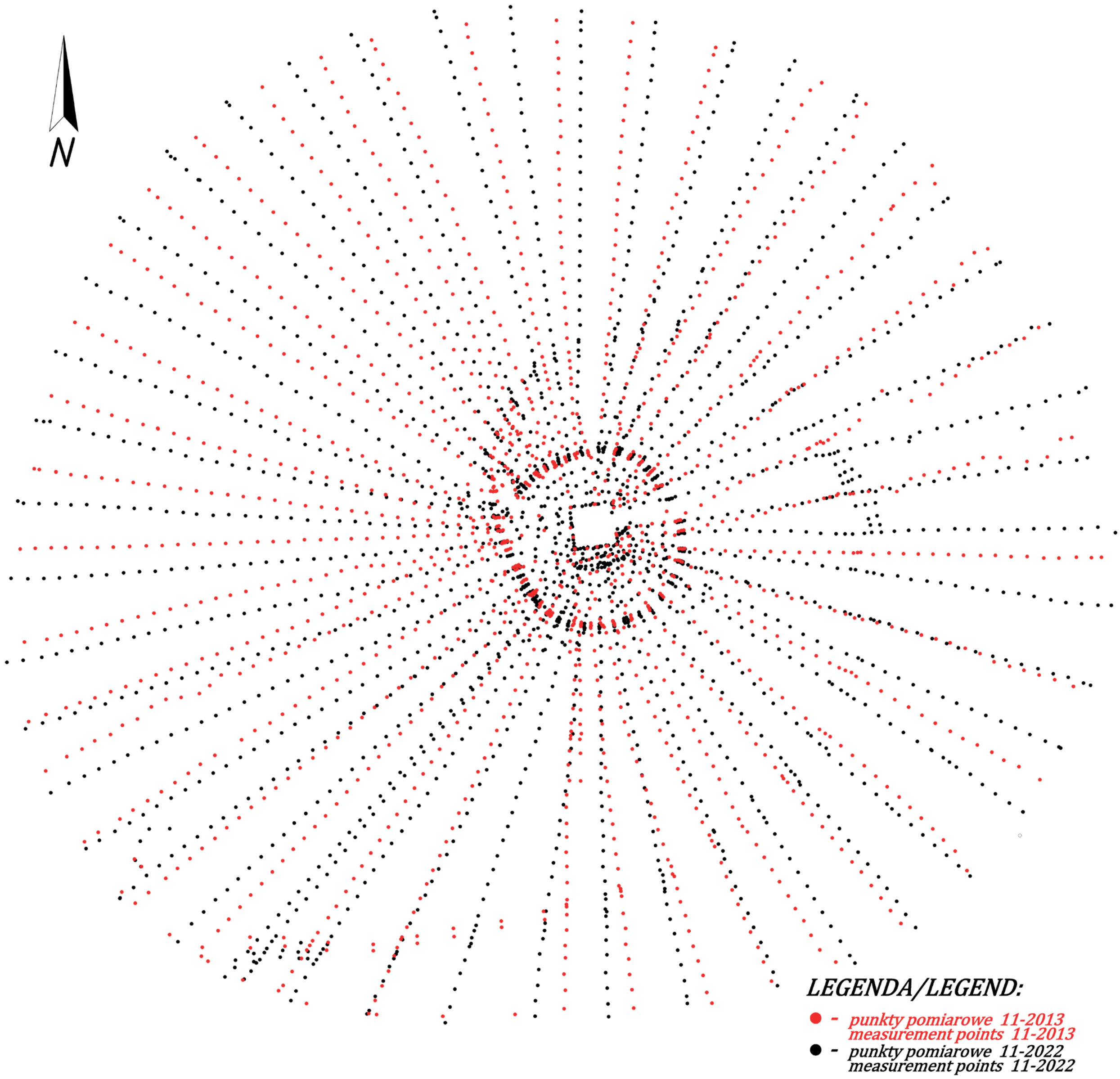

Fig. 7. Rozmieszczenie punktów pomiarowych w profilach – pomiary 2013 i 2022 r.
Ryc. 7. Distribution of measurement points in profile – measurements 2013 and 2022

verge of the base – 1.34 m and the path – 1.29 m. Almost the whole length of the spiral path was dislocated by the value of several decimetres. This also refers to the edge of the viewing gallery made of stone blocks. The biggest changes occurred in directions: N – 0.17 m, SSE – 0.16 m and SSW – 0.13 m (figure 8).

The carried-out measurements in the 9 years' interval, in the form of the profile lines allowed to define the directions and values of earth creep, which manifests in the dislocation of the spiral path into the top and stone belt around the viewing gallery. Relatively uniform distribution of profiles in both measurement series and similar number of points XYH provided reliable comparative material. Generated hypsometric maps of slopes (figure 9 – November 2022 and figure 10 – November 2022), emphasized zones of change in the inclination, especially in the vicinity of a spiral earth path, over and under its edges. The growth of the slope of

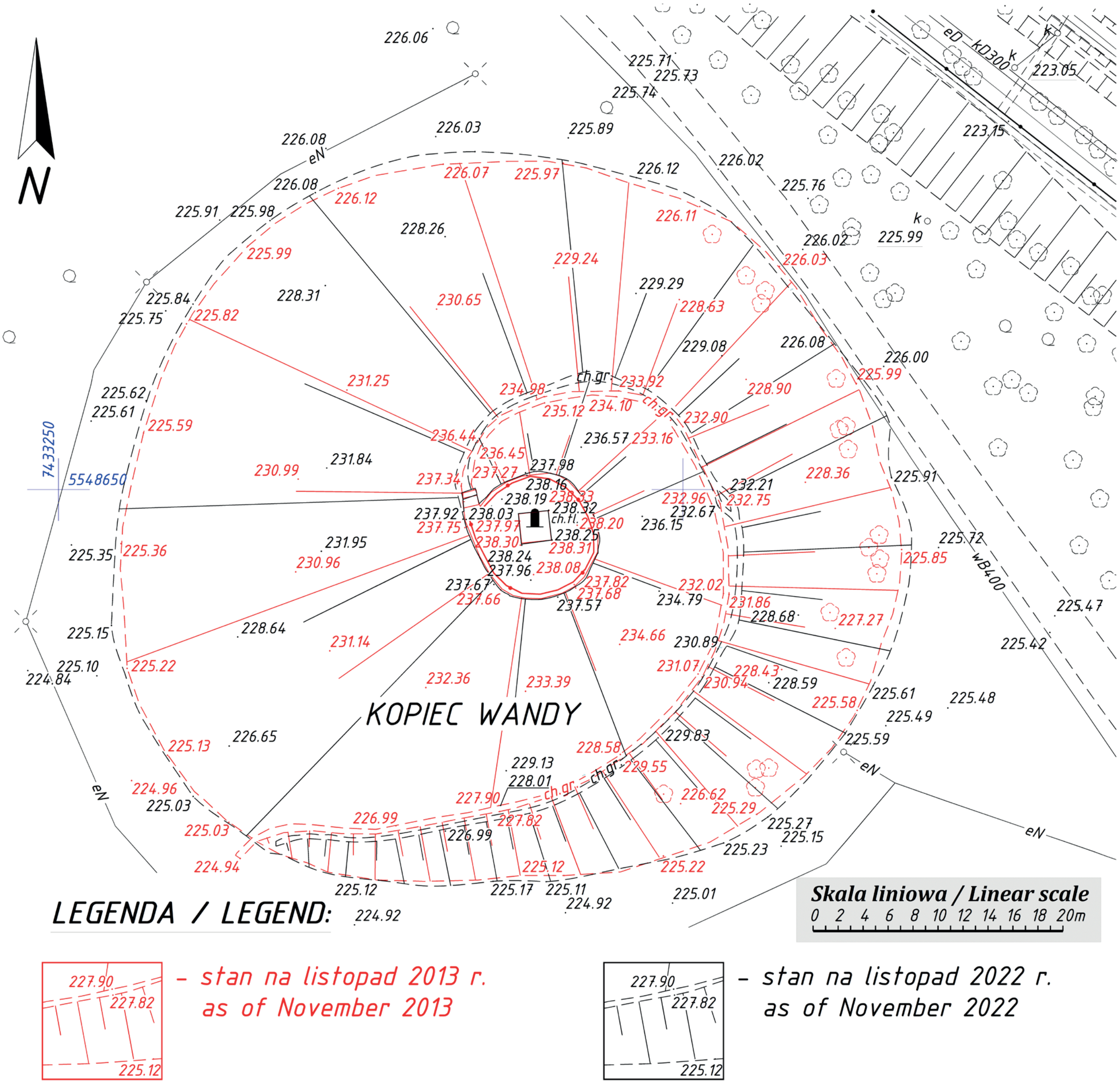

Fig. 8. Comparison of basic maps of the Wanda Mound area, the state of November 2013 and November 2022
Ryc. 8. Porównanie map zasadniczych obszaru Kopca Wandy według stanów na: XI.2013 r. oraz XI.2022 r.

scarps proves cumulation of earth masses as a result of creep and slide, observed in the southern and south-east side from September 2013. Distinct changes in the profile were recorded in south-west direction (profiles 1–3) and north-west (profiles: 25–26), where cumulations of earth masses occurred near the base of the mound and path (profile 25, 26) and in the perpendicular direction at the base – profiles 15–17). In the south-east direction near the edge of gallery, a zone of flattening of the earth top was formed and the growth of the values of scarp inclination, as well as the increase of its range occurred, what testifies about the activity of the landslide in this part of the mound. In the analysed interval of 9 years the points of the control network stabilized on the mound surface also showed the spatial movement of the earth masses.

The application of informatic-mathematic-graphic tools in AutoCAD, give the user possibility to con-

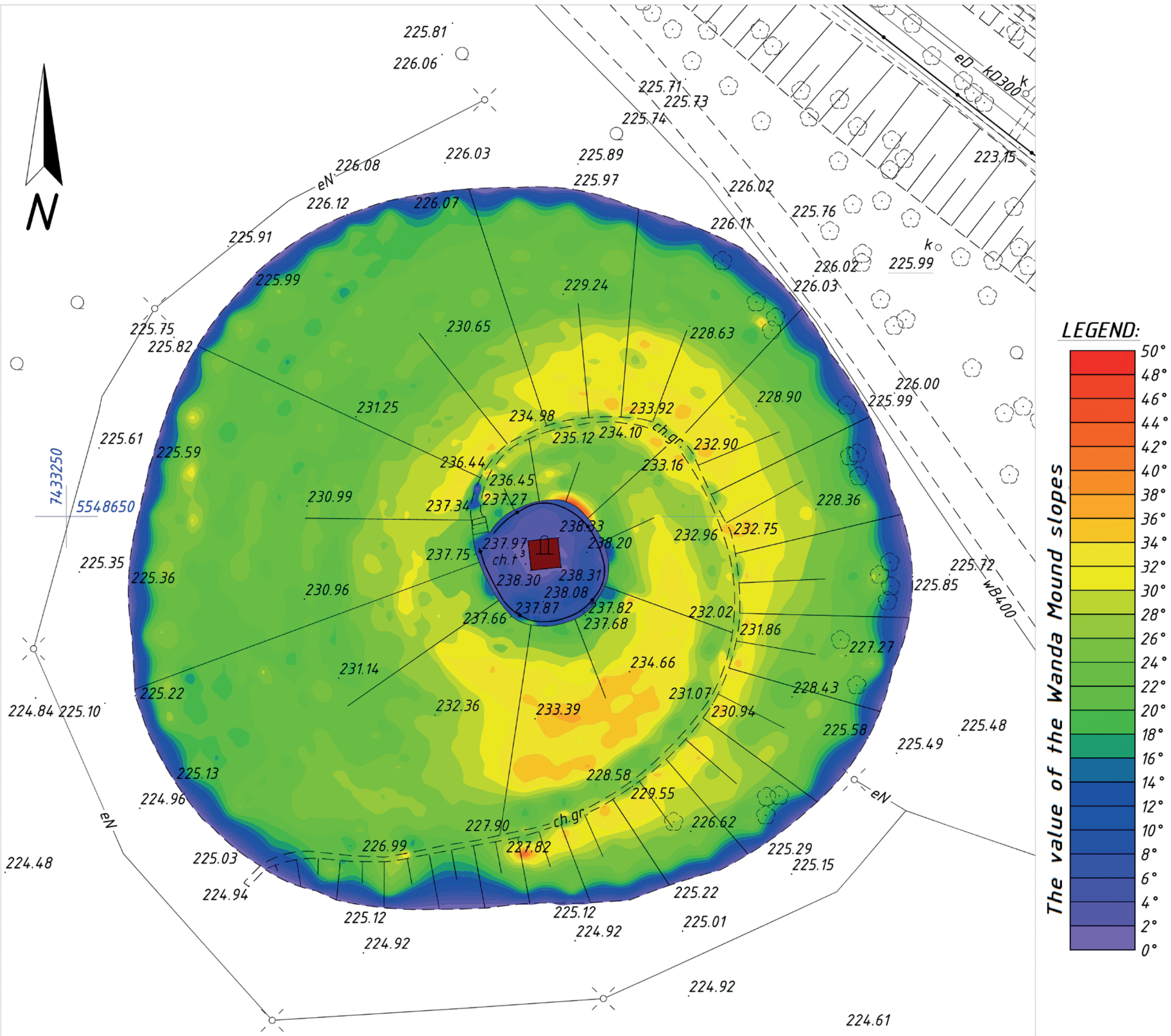

Fig. 9. Hypsometric map of the Wanda Mound slopes – November 2013
Ryc. 9. Mapa hipsometryczna spadków powierzchni Kopca Wandy – stan na listopad 2013 r.

struct the 3D model and their visualization. The effect of changing the point model on the verge-shell in AutoCAD was illustrated in figure 11. As a result, the presented in fig. 11 shell model (November 2022) was constructed in 1238 interpolation networks (Coons patches and 20 supplementing regions). Analysis of point data in both measurement series and generated cartographic documents in format 2D and 3D, allows parametrization of the object in the studied periods of the object functioning. It also makes a valuable material for the studies to mark the directions of geometric changes based on the analysis of selected morphometric parameters of the mound. Basic morphometric parameters of the Wanda Mound according to the state of November 2013 and November 2022 were presented in table 2.

Comparison of two independent 3D models allows visualization of geometric changes of the earth cover in the analysed period. Figure 12 illustrates geometric changes of the mound in the interval 2013–2022, presented in various perspectives. They show that in the north-east and south-east zone over the spiral path the most intense earth creep occurred, which contributed to horizontal dislocation in 0.6–1.29 m interval. The highest cumulation of the ground manifested at the base of earth monument from the western, south-west and south-east side. Around concrete-stone gallery a significant subsidence on the top of the mound.

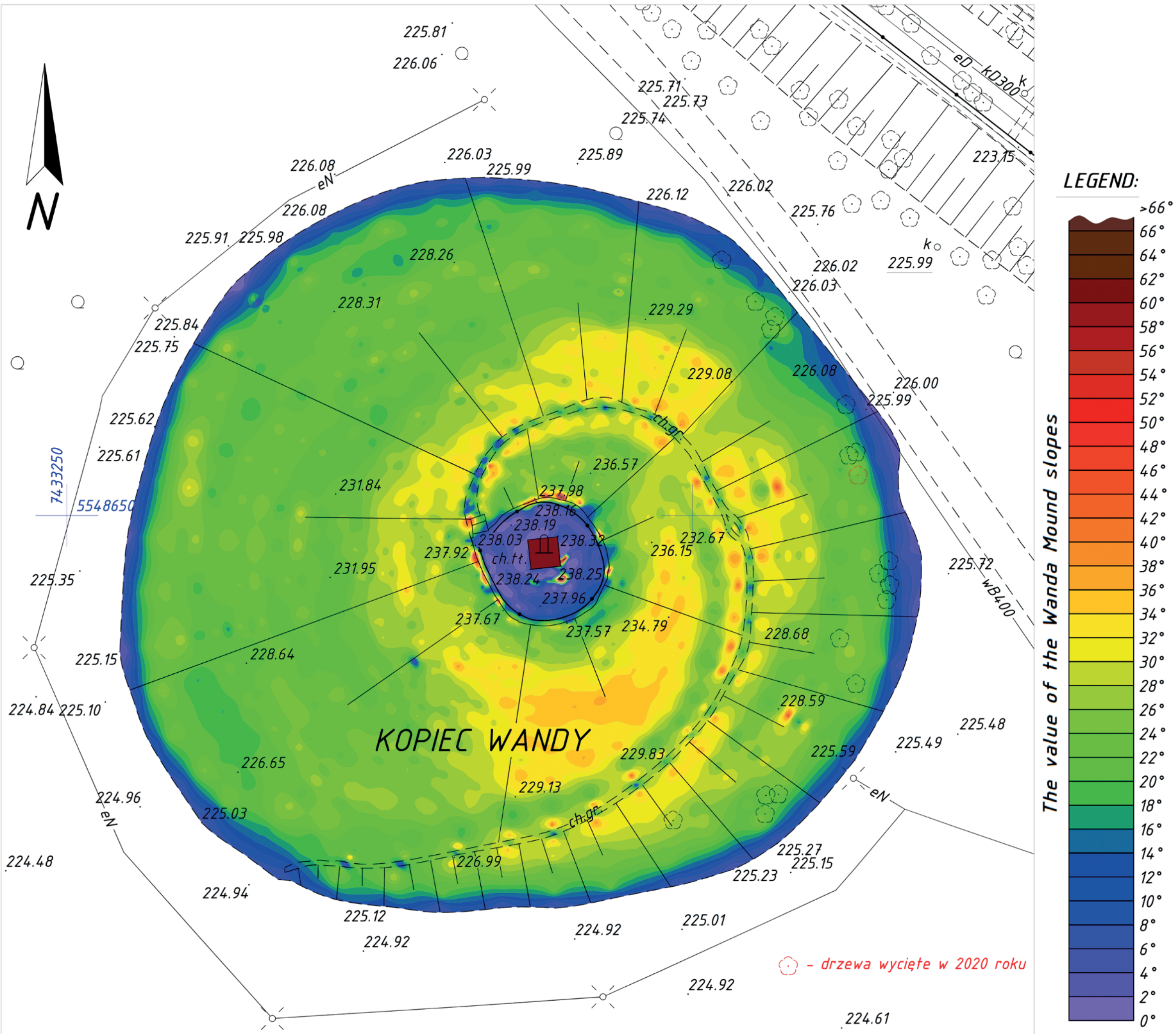

Fig. 10. Hypsometric map of the slopes of the Wanda Mound – November 2022
Ryc. 10. Mapa hipsometryczna spadków powierzchni Kopca Wandy – stan na listopad 2022 r.

Table 2. Basic morphometric parameters of the Wanda Mound November 11.2013 and 11.2022
Tabela 2. Zestawienie podstawowych parametrów morfometrycznych Kopca Wandy według stanów na: 11.2013 i 11.2022 r.

	Parameter	November 2013	November 2022
Base and scarps	Area of the base	2910.49	2989.08
	Perimeter of the base	192.03	195.10
	Maximal ordinate of the base [m AMSL]	226.15	226.12
	Minimal ordinate of the base [m AMSL]	224.99	225.03
	Maximal slope	49.9	70.7
	Minimal slope	0.2	0.1
	Mean slope	25.5	25.0
	Maximal radius [m] / Azimuth [°]	62.87 / 65°57’	64.44 / 73°01’
	Minimal radius [m] / Azimuth [°]	57.16 / 358°03’	57.89 / 5°38’

Table 2 cont. / **Tabela 2** cd.

	Parameter	November 2013	November 2022
Gallery	Area of the gallery	80.16	82.03
Gallery	Perimeter of the gallery w [m]	31.59	33.16
Gallery	Maximal ordinate of the gallery [m AMSL]	238.34	238.34
Gallery	Minimal ordinate of the gallery [m AMSL]	237.76	237.67
Gallery	Maximal slope	23.4	80.6
Gallery	Minimal slope	0.6	0.1
Gallery	Mean slope	5.6	22.4
Gallery	Maximal radius [m] / Azimuth [°]	10.22 / 14°01’	10.27 / 2°14’
Gallery	Minimal radius [m] / Azimuth [°]	9.53 / 57°38’	10.01 / 38°51’
	Number of points in the model	1733	2105
	Number of measurement profiles	38	45

a)

b)

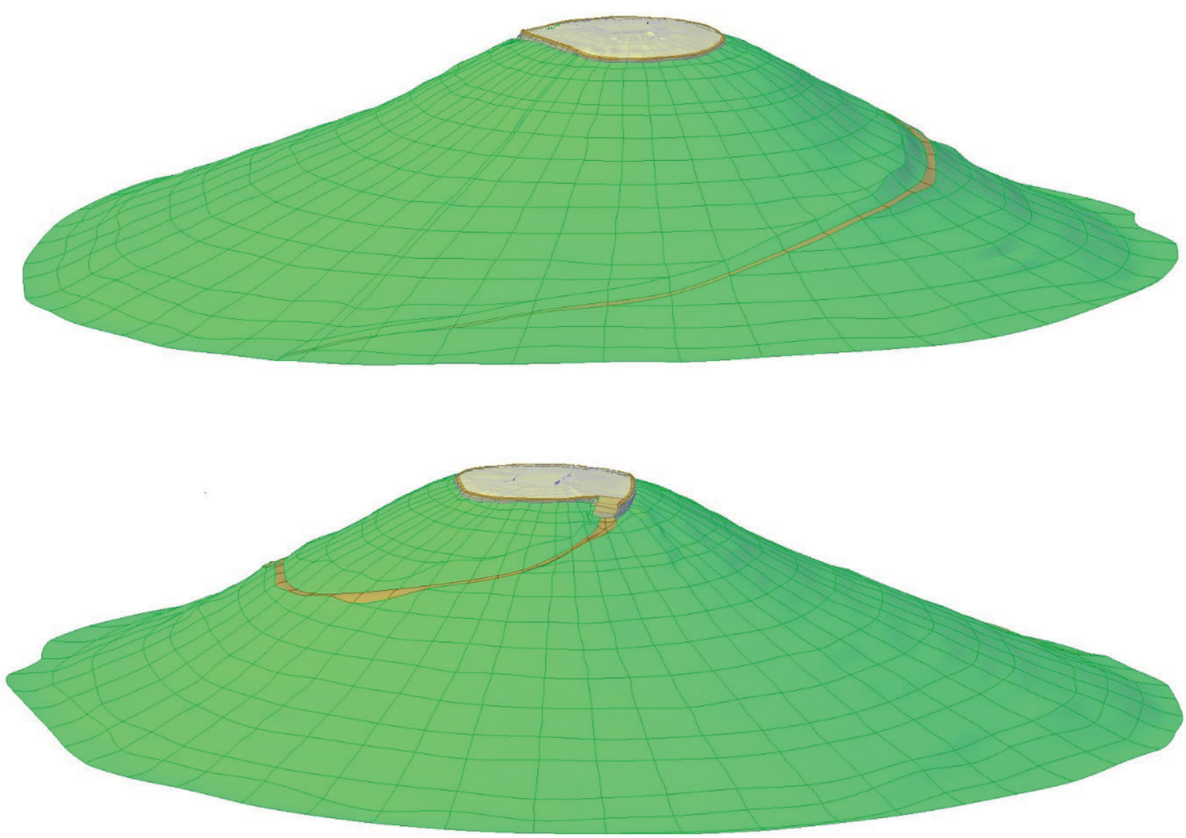

Fig. 11. 3D shell model of the Wanda Mound constructed from the splines and Coons patches and regions in AutoCAD (a – SW, b –N)

Ryc. 11. Powłokowy model trójwymiarowy Kopca Wandy zbudowany ze splajnów i płatów Coons’a oraz regionów w programie AutoCAD (a – od SW, b – od N) a)

b)

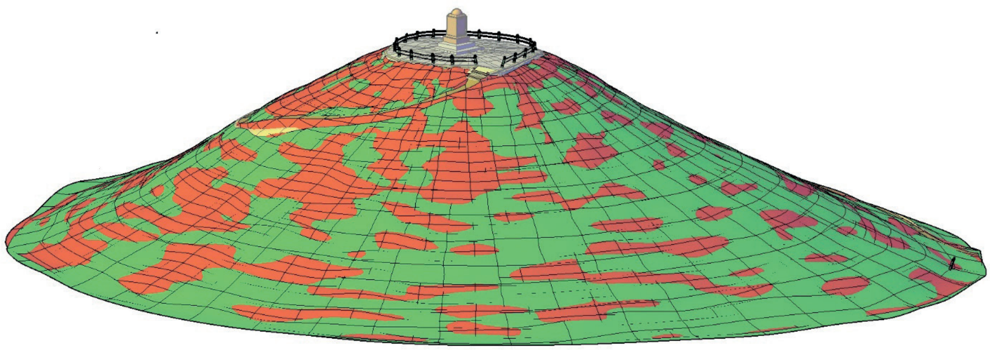

c)

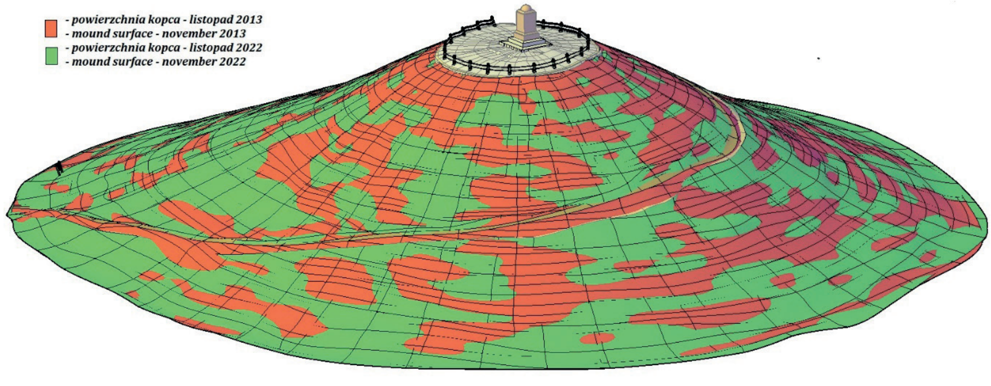

Fig. 12. Comparison of the 3D models of the Mound – November 2013 and November 2022 (views: a –from above; b – from NW; c – view from S-E)

Ryc. 12. Porównanie modeli trójwymiarowych Kopca według stanów na listopad 2013 i listopad 2022 (widoki: a – z góry; b – od NW; c – od SE)

5. CONCLUSIONS

The presented measurement and calculation-graphic procedures prove that electronic total stations with the use of the active signal and popular among engineers calculation software GeoNET and graphical software AutoCAD, gives wide spectrum of opportunities in term of the creation of 3D models and the analysis of geological threat (AutoCAD, Surfer).

The advantage of the presented measurement and graphic scheme based on the repetitiveness of the measurement at the reduction in the number of surveyors to one person and the way of constructing a model with the application of splines and interpolation networks, it is possible to define geometric structural changes in the Wanda Mound.

Simple and available mathematical and graphic tools (functions) contained in popular software in a basic version of AutoCAD type, facilitate the change of point shell or solid models and their visualization.

Using airborne technologies, at the data processing stage, requires the application of specialist calculation and graphic programs dedicated to a concrete group of measurement sets. Quite often the software is expensive and requires complex and complicated service. Modern software, connected with the measurement technology provides users very valuable data and final cartographic products. One must not forget that at the use of simpler tools, such as robotic total station, combined with mathematical and graphical abilities of the programs of CAD, environment, the user can obtain valuable data of high accuracy. Nowadays there is a possibility to convert these data into cartographic documents (maps, cross-sections, profiles, 3D models) and precise parametrization of the measured object. The results of the analysis indicate that RMSE error, which is in the best way describes the geometry of the model, settles on the level m=±39.4mm (without corrections based on control data). The control measurement based on dispersed points 232 indicated zones of values exceeding limiting error ±3 m (1.7% of all observations). In fact the regions of great changes refer to fragments of highly folded slopes (the amplitude can be up to several centimetres on significantly damaged surface) on a small space or zones close to the trees near the trees overgrowing the slope in the south east and east (local elevation of the ground by root systems), which was recorded during the control management. Thus the correction of the model can be carried out based on detail profiles or additional profiles situated in zones of growths in the values of modelling errors. Also the points of the control measurements can make a perfect fundament for the correction of the model geometry which will be the future base of the reference for subsequent states of the repetitively inventoried object.

The edge-network model is an easily edited product, allowing the introduction of small corrections at the stage of obtaining data. This makes a valuable comparative material in the future.

ACKNOWLEDGEMENTS

I wish to give my special thanks to Geosurvey for their technological support during the fieldwork in this study.

REFERENCES

1. Wojciechowski, T.; Laskowicz, I.; Kos, J.; Marciniec, P.; Uścinowicz, G.; Karkowska, K.; Przyłucka, M.; Wódka, M. Zagrożenia geologiczne w Polsce w 2021 r, Przegląd Geologiczny vol. 70, nr 9, 2021; pp. 617–626.
2. Perski, Z. Earth's Surface deformation measurements with SAR interferometry, methods and newest archivements. Geoinformatica Polonica nr 9, 2009; pp. 79–92.
3. Tukaj, R. Dokładność opracowań z wykorzystaniem pomiaru metodą skaningu laserowego – LIDAR, STANDARD ASPRS. Archiwum Fotogrametrii, Kartografii i Teledetekcji, vol. 15, Kraków 2004; pp. 41–47.
4. Toś, C.; Wolski, B.; Zielina, L. Geodezyjny monitoring zabytkowej budowli ziemnej metodą skaningu laserowego, Czasopismo Techniczne Budownictwo, zeszyt 9, 2008; pp. 247–354.
5. Gawałkiewicz, R. Wykorzystanie nowoczesnych technologii geodezyjnych w inwentaryzacji kopca Józefa Piłsudskiego. Półrocznik Sowiniec nr 42, Wydawnictwo Komitet Opieki nad Kopcem Józefa Piłsudskiego TMHiZK, 2013; pp. 63–94.
6. Szafarczyk, A.; Gawałkiewicz, R. Case study of the tensor analysis of ground deformations evaluated from geodetic measurements in a landslide area. Acta Geodynamica et Geomaterialia, vol. 13 no 2 (182), 2016; pp.213–222.
7. Borowiecki, I.; Michalik, A. Klasyfikacja chmury punków lotniczego skaningu laserowego z zastosowaniem programów TILTAN TLID, TERRASCAN VRMESH. Infrastruktura i Ekologia Terenów Wiejskich. Komisja Technicznej Infrastruktury Wsi, nr 1/III/2012 Polska Akademia Nauk – Oddział w Krakowie 2012; pp. 219–230.
8. Maciaszek, J.; Gawałkiewicz, R.; Szafarczyk, A. Geodezyjne metody badania osuwisk. Wydawnictwa AGH, Kraków 2013.

9. Kurczyński, Z.; Strojek, E.; Cisło-Lesicka, U. Zadania GUGiK realizowane w ramach projektu ISOK. Podręcznik dla uczestników szkoleń z wykorzystania produktów LiDAR – praca zbiorowa pod redakcją Piotra Wężyka. Warszawa 2015; pp. 22–58.
10. Borowiecki, I.; Ślusarski, M. Lotniczy skaning laserowy LIDAR miasta Krakowa (ocena dokładnościowa) – Infrastruktura i Ekologia Terenów Wiejskich, nr 3. Polska Akademia Nauk – Oddział w Krakowie, 2010; pp. 127–137.
11. Borowiecki, I. Analiza dokładnościowa lotniczego skaningu laserowego na obiekcie Wzgórze Wawelskie. ГЕОДЕЗІЯ, КАРТОГРАФІЯ І АЕРОФОТОЗНІМАННЯ – УКРАЇНСЬКИЙ МІЖВІДОМЧИЙ НАУКОВО-ТЕХНІЧНИЙ ЗБІРНИК, Вип. 68, Львів 2007; pp. 221–228.
12. Toś, C.; Wolski, B.; Zielina, L. Inwentaryzacja obiektu geotechnicznego na przykładzie Kopca im. J. Piłsudskiego w Krakowie, Górnictwo i Geoinżynieria, Rok 32, zeszyt 2, 2008; pp. 297–305.
13. Gawałkiewicz. R. Metodyka pomiaru i obróbki danych skaningowych w procesie modelowania na przykładzie inwentaryzacji zabytkowego Kopca Krakusa, Przegląd Budowlany, tom 7–8, Rok 78, 2006; pp. 60–68.
14. Lenda, G. Metody tworzenia i modyfikacji funkcji sklejanych na potrzeby opisu kształtu obiektów obserwowanych punktowo, Zeszyty Geodezja, tom 12, zeszyt 2/1, 2006; pp. 277–290.
15. Lenda, G. Using spline functions for the shape description of the Surface of shell structures. Geoinformatica Polonica, nr 13, 2014; pp. 21–32.
16. Kiciak, P. Podstawy modelowania krzywych i powierzchni: zastosowania w grafice komputerowej. Wydawnictwa Naukowo-Techniczne, 2000.